Peer-reviewed version available at *Fibers* **2020**, *8*, 30; doi:10.3390/fib8050030

Review

Laser Sources Based on Rare-Earth Ion Doped Tellurite Glass Fibers and Microspheres

Elena A. Anashkina

Federal Research Center Institute of Applied Physics of the Russian Academy of Sciences, 46 Ul'yanov Street, 603950 Nizhny Novgorod, Russia; elena.anashkina@ipfran.ru

Abstract: In recent years, tremendous progress has been made in the development of rare-earth ion doped tellurite glass laser sources, ranging from watt and multiwatt level fiber lasers to nanowatt level microsphere lasers. Significant success has been achieved in extending the spectral range of tellurite fiber lasers generating at wavelengths beyond 2 μm as well as in theoretical understanding. This review is aimed at discussing the state of the art of neodymium-, erbium-, thulium-, and holmium-doped tellurite glass fiber and microsphere lasers.

Keywords: tellurite fiber laser; tellurite glass fiber; microlaser; microsphere laser; rare-earth ions

1. Introduction

Tellurite glasses (based on tellurium dioxide TeO_2) possess chemical stability, have a broad transmission range of ~0.4-6 μm, high linear ($n \sim 1.8$-2.3) and nonlinear refractive indices, and relatively low phonon energies (~700-900 cm^{-1}) [1-9]. Many compositions are resistant to crystallization. Detailed discussion of the physico-chemical properties of tellurite glasses can be found in the books [1,2]. Current technologies allow creating high-purity low-loss "ultra-dry" tellurite glasses and fibers [8,9], so with allowance for substantial solubility of rare-earth ions, tellurite glass-based rare-earth-doped elements as active media for laser sources seem very attractive [4,10]. Due to the high refractive index, the stimulated emission cross sections proportional to $(n^2+2)^2/9n$ for tellurite glasses are higher than for silica ones [10]. Low phonon energies allow operation in the spectral range well beyond 2 μm, expanding the possibilities of achieving longer wavelength generation in comparison with silica glass [11,12].

In addition to choosing the material of gain medium, when developing photonic devices, considerable attention should be paid to the geometry of active elements. Fibers and microspheres have significant benefits in this respect. Thanks to the exploitation of waveguide light propagation, fiber lasers have advantages such as high efficiency of converting pump energy into radiation energy, efficient heat removal, and high quality of the spatial profile of the laser beam. Cavities for tellurite fiber lasers can be formed by bulk mirrors, reflective coatings deposited on fiber ends, fiber ends themselves, or by their combinations. Additional optical elements such as lenses or beam splitters can be also placed into a laser cavity. An example of a possible fiber laser scheme is shown in Fig. 1.

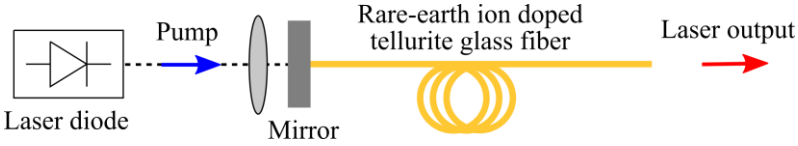

Figure 1. Variant of experimental fiber laser scheme with forward diode pumping using a mirror at the input fiber end and cleavage at the output end as a cavity.

Peer-reviewed version available at Fibers 2020, 8, 30; doi:10.3390/fib8050030

For microsphere-based lasers, which can be used as miniature photonic devices for basic science and many real applications, for example, for sensing [13], a gain medium and a cavity are the same device that is a microresonator with whispering gallery modes (WGMs) [14]. Such microresonators typically have high quality factors (Q-factors) and small optical mode volumes which make them suitable for constructing low threshold and narrow linewidth lasers [13,14]. For efficient excitation of WGMs, evanescent-wave coupling is required. Commonly, coupling can be implemented using a tapered fiber with a waist diameter meeting phase matching conditions [14]. Coupling can be also realized by means of a prism by adjusting the angle of incidence to achieve phase matching [15]. An example of a possible microsphere laser scheme is shown in Fig. 2.

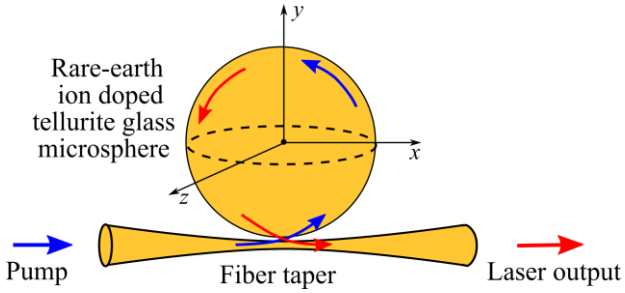

Figure 2. Variant of experimental microlaser scheme with a fiber taper used for both, pump coupling and extracting the generated radiation from the microsphere.

In this review we discuss laser sources utilising fibers and microspheres based on rare-earth-doped tellurite glasses. Lasing was attained at the radiative transitions of the following ions: Nd^{3+} [16-21], Er^{3+} [22-32], Tm^{3+} [11,12,33-46], and Ho^{3+} [47-56]. In most works on tellurite fiber and microsphere lasers, generation was achieved in a continuous wave (CW) regime. For tellurite fiber lasers, several works were devoted to pulsed generation including via Q-switch [28,38,48] or pulsed pump [12]. The generation of ultrashort pulses via mode-locking has not been reported yet for tellurite fiber and microsphere lasers. Note that in the book [1] there is the Chapter "Lasers Utilising Tellurite Glass-Based Gain Media"[10] on the same topic with references to the research works published in 2015 and earlier. But since 2015, significant progress has been made in the development of such laser sources, including achieving the watt and multiwatt level of laser radiation near 2 μm [52,53] and attaining generation in the range well above 2 μm in tellurite active elements [11,12]. Significant advances have been also achieved in the theory of such sources [8,11,29,53,56-59]. Therefore, this review is focused on the recent results. Nevertheless, an attempt of summarizing all the data on the reported tellurite glass fiber-based and microsphere-based lasers has also been made.

2. Neodymium

A rare-earth Nd^{3+} ion has an intensive absorption band near 800 nm corresponding to the wavelengths of low cost commercial laser diodes and Ti:sapphire lasers [10]. Therefore these laser sources are widely used for pumping Nd-doped gain media including tellurite glass based ones. Under pumping at a wavelength near 800 nm, Nd^{3+} ions are excited to the ($^4F_{5/2}$, $^2H_{9/2}$) states from the ground level $^4I_{9/2}$ via the ground state absorption. Next, rapid relaxation from short-lived ($^4F_{5/2}$, $^2H_{9/2}$) states to the upper laser level $^4F_{3/2}$ occurs due to non-radiative multiphonon decay. Further, the emission band of Nd^{3+} peaking at about 1060 nm can be observed due to the $^4F_{3/2} \rightarrow {}^4I_{11/2}$ transition. A simplified scheme of Nd^{3+} energy levels is shown in Fig. 3.

Note that Nd^{3+} ions can also be pumped at shorter wavelengths. For example, the first tellurite bulk glass-based laser operating near 1060 nm using Nd-doped sample pumped by an Argon laser at 514.5 nm was demonstrated in 1978 [60]. However, with the development of Ti:sapphire lasers and laser diodes, other pump sources for Nd-doped gain elements lost relevance.

Peer-reviewed version available at Fibers 2020, 8, 30; doi:10.3390/fib8050030

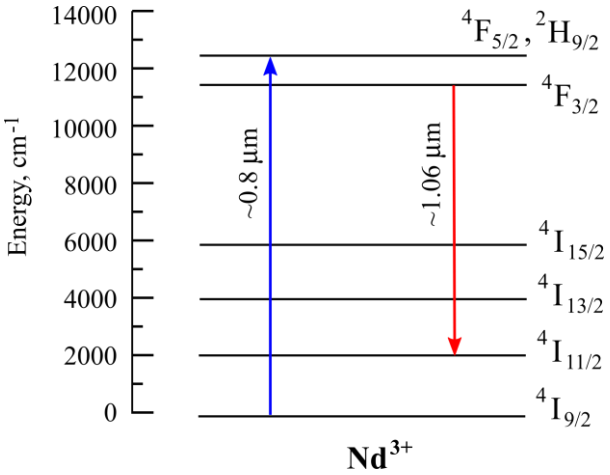

Figure 3. Simplified energy level diagram for Nd-doped tellurite glass.

2.1. Lasing in Nd-doped fibers

The first tellurite glass fiber laser was reported in 1994 [16]. A 0.6-m piece of fiber with $76.9TeO_2$-$6.0Na_2O$-$15.5ZnO$-$1.5Bi_2O_3$-$0.1Nd_2O_3$/$75TeO_2$-$5Na_2O$-$20ZnO$ core/cladding glass compositions was pumped by a Ti:sapphire laser at 818 nm. The fiber resonator was established by Fresnel reflection of 11.9% at both ends without external mirrors. The slope efficiency for the power output from one end of the fiber was 23% relative to pump power. Assuming equal emission from both ends, the slope efficiency above threshold was estimated to be 46%. The threshold was approximately 27 mW. Laser generation was single-modal for pumping above the threshold, and became multimodal for pumping well above the laser threshold. The maximal output power from one fiber end exceeded 4 mW [16].

2.2. Lasing in Nd-doped microspheres

Lasing in the ~1058-1075 nm range in Nd-doped tellurite microspheres using Ti:sapphire lasers for pumping was reported in several research works [17-21]. The first tellurite microlaser was demonstrated in 2002 [17]. The microsphere was produced by melting the end of a glass wire using a Kanthal wire heater [17]. The microsphere was pumped by a Ti:sapphire laser tuned to 800 nm. The incident beam was focused via a microscope objective lens so that the pump beam irradiated a point slightly offset from the center of the sphere. The output laser radiation at ~1.06 μm was collected using a multimode fiber. The microsphere laser with a diameter of 140 μm had an incident pump threshold of 81 mW, but pump coupling was not optimized [17].

In 2003, it was shown that the oscillation wavelength of a microlaser could be controllable using a $\lambda/4$-shifted distributed feedback resonator fabricated on the surface of a microsphere [18]. The lasing wavelength was in agreement with the Bragg wavelength of the grating estimated from the grating period and the effective index of WGMs. Tapered optical fibers were used for both, coupling the pump light and extracting the output radiation. The threshold of the laser based on a microsphere with a Q-factor of ~10^5 was lower than 40 mW. Single-mode and multimode generation was observed in the ~1058-1075 μm range for different sphere diameters of ~70-180 μm [18].

Bubble-containing Nd-doped tellurite glass microspheres were produced and investigated [21]. The localized laser heating technique was applied for sample fabrication. When the edge part of the 20-μm-microsphere with a 1.6-μm-bubble was pumped, periodic peaks caused by the WGMs were observed. However, when the bubble position was pumped, not only WGMs but also a continuous range of other wavelengths were excited. It was shown that the introduction of a bubble into the microresonator induces “non-WGM excitation,” lowering the lasing threshold. The lowest observed lasing threshold was 34 μW for the bubble-containing microsphere with a diameter of 4 μm, which agreed with the theoretical estimations [21].

3. Erbium

Peer-reviewed version available at Fibers 2020, 8, 30; doi:10.3390/fib8050030

A rare-earth Er^{3+} ion has an absorption band near 980 nm corresponding to the wavelengths of low cost commercial laser diodes which are standard telecom components. Radiation at ~980 nm via the ground state absorption from the $^4I_{15/2}$ level excites the $^4I_{11/2}$ level (see Fig. 4). After that, the transition from the $^4I_{11/2}$ to the $^4I_{13/2}$ level occurs. For silica glass, due to high phonon energy, the $^4I_{11/2}$ level is depopulated non-radiatively, but for tellurite glasses, the radiative transition near the 2.7-2.8 μm range is possible [61]. After that, the $^4I_{13/2}$ level is populated and lasing in the 1.53-1.6 μm range at the $^4I_{13/2} \rightarrow {}^4I_{15/2}$ transition can be attained (see Fig. 4). So, tellurite glasses can be used as a gain medium for lasing in the 1.53-1.6 μm range as well as in the 2.7.2-8 μm range. For lasing in the 1.5 μm region, in-band pump by standard laser diodes at 1480 nm or silica fiber lasers can be also used. Er-doped tellurite fibers are promising for L-band amplifiers and lasers due to their larger stimulated emission cross-sections and lower excited-state absorption at longer wavelengths in comparison with Er-doped silica fibers [30].

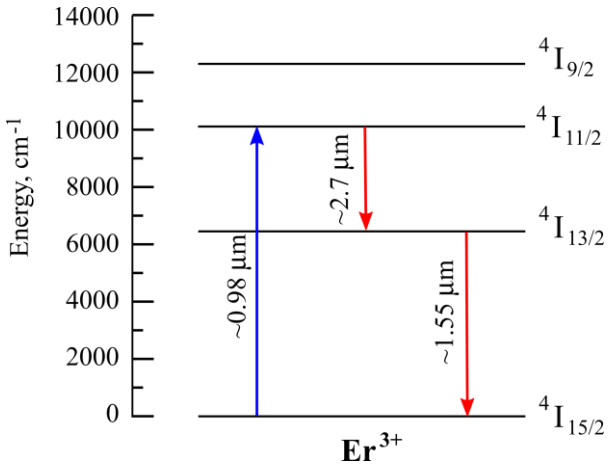

Figure 4. Simplified energy level diagram for Er-doped tellurite glass.

3.1. Lasing in the 1.5 μm region in Er-doped fibers

The first signal amplification and laser oscillation at a wavelength of 1560 nm in Er-doped tellurite fibers was claimed in [22]. A small-signal gain of 16 dB was obtained for a pump power of 130 mW at 978 nm. A laser oscillation was observed with a threshold pump power of 120 mW at 978 nm and a slope efficiency of 0.65% in a 85-cm fiber. A fiber cavity was based on the Fresnel reflection of 12.3% at both ends, without the use of dichroic mirrors [22]. Since then Er-doped tellurite fiber lasers have been developed and investigated [23-30].

A CW Er-doped zinc-tellurite fiber laser was recently reported in [29]. A single-mode generation was attained in a 20-cm long piece of fiber pumped by a single-mode laser diode at 975 nm. The pump wave was launched into the fiber core using a beam splitter put into a laser cavity which was formed by two aspheric lenses. Laser radiation at 1555 nm was extracted through the beam splitter [29].

L-band wavelength-tunable CW Er-doped tellurite fiber lasers were reported in [30]. A wavelength-tunable range of 38 nm from 1589 to 1627 nm was achieved with 3-m long TeO_2–ZnO–La_2O_3 glass based fiber pumped by a fiber laser at 1570 nm with a maximum output power of 2.5 W. A linear laser cavity contained a high reflection mirror, a fiber coupler, a wavelength division multiplexer, an active tellurite fiber, a collimation lens, and a diffraction grating. The wavelength tuning was realized with the Littrow configuration [30].

Self-Q-switching behavior of Er-doped tellurite microstructured fiber lasers was reported in [28]. At a pump power of 705 mW at 1480 nm, output laser pulses having a wavelength of 1558 nm, a repetition rate of 1.14 MHz, and a pulse width of 282 ns were generated from the 14-cm piece of the active fiber using a linear cavity. The maximum output power was 316 mW and the slope efficiency was about 72.6% before the saturation of the laser power. The authors explained the self-Q-switching behavior by the re-absorption originating from the ineffectively pumped part of the active fiber [28].

Peer-reviewed version available at Fibers 2020, 8, 30; doi:10.3390/fib8050030

A high-performance Er/Ce co-doped tellurite fiber amplifier and tunable fiber laser using a dual-pumping scheme at 980 nm and 1480 nm were presented in [23]. A 22-cm long piece of gain fiber in a fiber ring laser configuration was used to generate radiation with a tuning range of 83 nm (from 1527 to 1610 nm). The addition of Ce^{3+} co-doping with Er^{3+} was used for a resonant energy transfer from Er^{3+}: $^4I_{11/2} \rightarrow {}^4I_{13/2}$ to Ce^{3+}: $^2F_{5/2} \rightarrow {}^2F_{7/2}$, which reduced excited state absorption from the Er^{3+} $^4I_{11/2}$ level and improved the ~1.6 μm gain characteristics [23].

3.2. On the possibilities of lasing in the 2.7-2.8 μm region in Er-doped fibers

Luminescence in the 2.7-2.8-μm region at the $^4I_{11/2} \rightarrow {}^4I_{13/2}$ energy transition in tellurite glasses was first observed in [62] and was later reported by various research groups both, in glasses and in fibers [61,63-67]. However, master oscillators or amplifiers at 2.7-2.8 μm based on Er-doped tellurite glass fibers or other tellurite glass optical elements have not been published in refereed journals yet, but researches in this direction are conducted. One of the reasons for the absence of such lasers is the problem of strong absorption by hydroxyl groups in the range of interest. The second reason is that the lifetime τ_3 of the $^4I_{11/2}$ energy level is significantly shorter than the lifetime τ_2 of the $^4I_{13/2}$ level due to relatively high phonon energy (~750 cm^{-1} for zinc-modified tellurite glasses and ~900 cm^{-1} for tugsten-modified tellurite glasses [1]). For zinc-tellurite glasses, τ_3 is about 200-300 μs [29,61,67] but for tugsten-tllurite glasses τ_3 is about 100 μs [8], whereas τ_2 reaches a few ms for different glass compositions [29,61]. This leads to high population of the $^4I_{13/2}$ level and low population of the $^4I_{13/2}$ level under continuous wave (CW) pump at the $^4I_{15/2} \rightarrow {}^4I_{11/2}$ transition. A possible solution of the first problem is to produce high-quality "ultra-dry" TeO_2-based samples [8]. To overcome the second challenge and populate effectively the $^4I_{11/2}$ level, different ways shown schematically in Fig. 5 were proposed. These include:

1. Using very high Er^{3+} ion concentrations providing a high up-conversion rate ($^4I_{13/2} + {}^4I_{13/2} \rightarrow {}^4I_{9/2} + {}^4I_{15/2}$) (see Fig. 5(a)) [61,66].
2. Using pulsed pump with a duration of order τ_3 and a repetition rate lower than $1/\tau_2$ (see Fig. 5(b)) [8].
3. Using dual-wavelength cascade laser schemes at two consecutive radiative transitions $^4I_{11/2} \rightarrow {}^4I_{13/2}$ and $^4I_{13/2} \rightarrow {}^4I_{15/2}$ at 1.56 and 2.8 μm, respectively, see Fig. 5(c) [29].
4. Using two-color pump schemes with the first pump wavelength of 0.98 μm ($^4I_{15/2} \rightarrow {}^4I_{11/2}$) or 1.56 μm ($^4I_{15/2} \rightarrow {}^4I_{13/2}$) and the second pump wavelength of 1.7 μm ($^4I_{13/2} \rightarrow {}^4I_{9/2}$) (see Fig. 5(d)) [59].

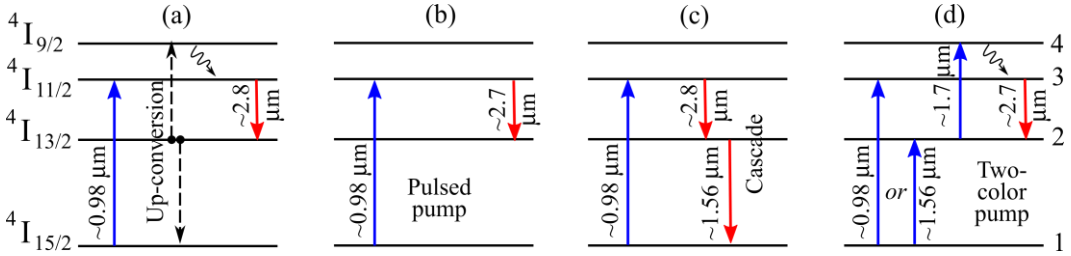

Figure 5. Schematic of different ways of effective population of the $^4I_{11/2}$ level of Er^{3+} ions in tellurite glasses. (a) 1. Up-conversion for very high Er^{3+} ion concentrations. (b) 2. Pulsed pump. (c) 3. Dual-wavelength cascade lasing. (d) 4. Two-color pump.

Regarding the first way, it was proposed to effectively depopulate the level $^4I_{13/2}$ and populate the level $^4I_{11/2}$ exploiting energy transfer up-conversion processes [61]. It was found experimentally that energy transfer rate parameters strongly depend on Er^{3+} ion concentration [61]. The higher Er^{3+} content, the larger up-conversion rate is [61]. On the basis of experimental data, it was calculated that for Er^{3+} concentration $>1.2 \cdot 10^{21}$ cm^{-3} (or Er_2O_3 ~2.65 mol. % for zinc-telurite glass) and OH^- concentration equal to zero, a population inversion was determined for a threshold pumping intensity of ~87 kW/cm^2 at 976 nm [61]. The first theoretical analysis of ultrashort pulse amplification in the 2.7-3 μm range under diode pumping at 975 nm was performed in [66]. The possibility of

Peer-reviewed version available at Fibers 2020, 8, 30; doi:10.3390/fib8050030

producing pulses with the energy of ~10 nJ and the duration smaller than 100 fs with ~20 dB gain was shown numerically for fibers manufactured from high-purity TeO_2–ZnO–La_2O_3–Na_2O glasses with 10^{21} cm^{-3} concentration of erbium ions in the core and a low content of hydroxyl groups [66].

As concerns the second way, a possibility of realizing a diode-pumped gain-switched laser with 100 Hz repetition rate based on specially developed Er-doped single-mode and multi-mode TeO_2-WO_3-La_2O_3-Bi_2O_3 glass fibers was proposed and investigated in [8]. When the pump is switched on, the upper laser level $^4I_{11/2}$ starts to be populated. The initial population of the $^4I_{13/2}$ level is zero. Laser oscillating starts to develop when the threshold is reached. It is determined from the condition that the signal gain for a cavity round trip is comparable to the total losses including the linear fiber loss and the loss of radiation output from the cavity. When the first pump pulse is applied, the population n_3 of the level $^4I_{11/2}$ starts to increase linearly with time. At the moment of spike generation, n_3 decreases and the population n_2 of the level $^4I_{13/2}$ increases by the corresponding value. When the duration of the pump pulse is comparable to τ_3, the depopulation of the upper level $^4I_{11/2}$ due to spontaneous nonradiative transitions becomes significant. But the population of the $^4I_{13/2}$ level with a lifetime of several ms continues to increase. The efficiency of generation decreases until complete disappearance. Therefore, the pump duration should be chosen around τ_3. After this, the residual population relaxes from the $^4I_{11/2}$ level to the $^4I_{13/2}$ level with a characteristic lifetime τ_3. Relaxation from the $^4I_{13/2}$ level to the ground state $^4I_{15/2}$ occurs with a characteristic time $\tau_2 >> \tau_3$. Therefore, the repetition rate of the pump pulses should be low enough for the vast majority of the excited ions to have sufficient time to transit from the $^4I_{13/2}$ level to the ground state by the time of the second pump pulse arrival [8].

The third opportunity concerns using dual-wavelength cascade laser schemes at 1.56 μm and 2.8 μm (which was demonstrated for fluoride fiber lasers doped with Er^{3+} ions with 50% slope efficiency at 2.8 μm exceeding the Stokes limit by 15% [68]). The first theoretical analysis of such a scheme for Er-doped tellurite fibers was performed in the paper [29]. A numerical model calibrated to the experimental data (concerning laser generation and amplification at 1.555 μm in TeO_2–ZnO–La_2O_3–Na_2O glass fibers doped with 0.24 mol.% Er_2O_3 [29]) for prediction and optimization of laser characteristics in schemes with different parameters was developed [29]. The model describes single-wavelength lasing as well as dual-wavelength cascade lasing at 1.555 μm and 2.8 μm. It was shown numerically that for the optimized parameters, the maximum slope efficiency at 2.8 μm at the $^4I_{11/2} \rightarrow {}^4I_{13/2}$ transition can reach ~20%. The maximum calculated efficiency at 1.555 μm exceeds 30%.

For the fourth opportunity based on using two-color pump schemes with the first pump wavelength of 0.98 μm ($^4I_{15/2} \rightarrow {}^4I_{11/2}$) or 1.56 μm ($^4I_{15/2} \rightarrow {}^4I_{13/2}$) and the second pump wavelength of 1.7 μm ($^4I_{13/2} \rightarrow {}^4I_{9/2}$), the metastable level $^4I_{13/2}$ is a "virtual ground state" [59]. The first pump populates the $^4I_{13/2}$ level, and the second pump at a wavelength of 1.7 μm is needed to transfer ions from $^4I_{13/2}$ to the short-lived energy level $^4I_{9/2}$, from which a rapid non-radiative relaxation to the operating level $^4I_{11/2}$ occurs. The theoretical investigation of lasing at the $^4I_{11/2} \rightarrow {}^4I_{13/2}$ energy transition under two-color pump on the basis of the experimentally measured parameters of an Er-doped core tellurite fiber from TeO_2-ZnO-La_2O_3-Na_2O glass with the concentration of Er^{3+} ions of $N_{Er} = 10^{20}$ cm^{-3} was performed in [59]. It was shown numerically that, for an optimal fiber length, the small-signal gain may exceed 18 dB and laser generation may be achieved with a relatively low threshold of a few hundreds of mW and a maximum slope efficiency can reach ~ 40% [59].

Note that for numerical modelling of different schemes of Er-doped and other rare-earth ion-doped fiber lasers, full systems of equations, corresponding approaches and methods for their solution were presented and described in [69-73].

3.3. Lasing in Er-doped microspheres

Lasing in Er-doped tellurite microspheres have been demonstrated only at the $^4I_{13/2} \rightarrow {}^4I_{15/2}$ energy transition using 975-nm pump at the $^4I_{15/2} \rightarrow {}^4I_{11/2}$ transition [31] and using 1480-nm in-band pump at the $^4I_{15/2} \rightarrow {}^4I_{13/2}$ transition [32]. Microspheres were fabricated and investigated by the same research group [31,32]. A spin method was applied for fabrication. Tellurite glass was melted in a

Peer-reviewed version available at Fibers 2020, 8, 30; doi:10.3390/fib8050030

furnace and dropped on a spinning plate. The melted glass was spun out by centrifugal force and cooled down quickly, forming microspheres with diameters from a few μm to a few hundred μm by surface tension [31,32]. The Q-factors were estimated to be 10^5-10^6 [31,32] and $3 \cdot 10^6$ [32]. A silica fiber taper was used for both, pump coupling and extracting the generated radiation from microspheres. The generation was achieved in the 1560–1610 nm range by adjustment of pump power [31]. By tuning the contact position between the fiber taper and the microsphere and selecting the microsphere size, single-mode as well as multimode lasing in the L-band was reached [31]. The temperature dependence of the wavelength and the laser threshold was also studied in [32]. The wavelength tuning in the ~1606-1608 nm range was experimentally demonstrated and theoretically confirmed by taking into account the thermal expansion of the tellurite glass. It was shown that the threshold increased with temperature [32].

4. Thulium

A rare-earth Tm^{3+} ion in tellurite glass matrixes has several radiative transitions at the $^3F_4 \rightarrow {}^3H_6$ transition in the 1.9-2 μm range, at the $^3H_4 \rightarrow {}^3H_5$ transition near 2.3 μm, and at the $^3H_4 \rightarrow {}^3F_4$ transition near 1.5 μm as shown in Fig. 6. To achieve generation at these transitions, pumping by commercial laser diodes at ~800 nm can be used to excite the $^3H_4$ level from the ground level $^3H_6$ via the ground state absorption at the $^3H_6 \rightarrow {}^3H_4$ transition. To achieve generation only in the 1.9-2 μm range, in-band fiber laser pump near 1.6 μm can be used effectively.

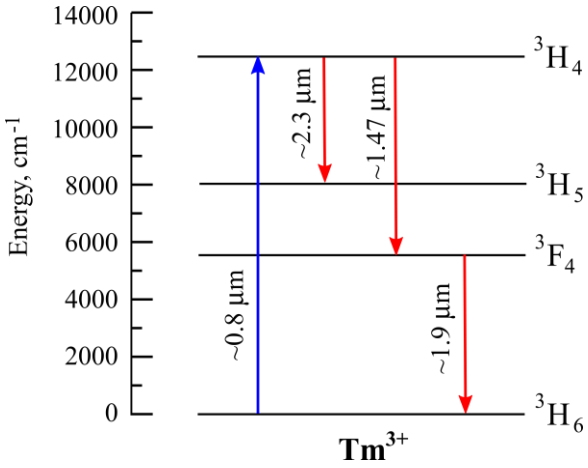

Figure 6. Simplified energy level diagram for Tm-doped tellurite glass.

4.1. Lasing in the 1.9-2 μm range in Tm-doped fibers

The first Tm-doped tellurite fiber laser was reported in [33]. The generation in the 1.88–1.99 μm range was demonstrated in a 32 cm long fiber with core composition of $80TeO_2$–$10ZnO$–$10Na_2O$ mol.% co-doped with 1.0 wt.% Tm_2O_3 and 1.5 wt.% Yb_2O_3, and the cladding composition of $75TeO_2$–$15ZnO$–$10Na_2O$ mol.%. The laser cavity was constructed using a high reflectivity mirror at the pump end and 12% Fresnel reflection at the output fiber end. The tellurite fibers were in-band pumped by an Er^{3+}/Yb^{3+}-doped silica fiber laser operating in the 1.57–1.61 μm range. The maximum obtained slope efficiency of 76% was very close to the Stokes efficiency limit of ~82%. The maximum output power of 280 mW was a record one for tellurite fiber lasers [33].

In the further studies of Tm-doped tellurite fiber lasers, an increase in output power to ~0.4 W with in-band pump [40] and to ~0.5 W [36] and 1.12 W [35] with laser diode pump at ~0.8 μm was obtained. A watt level CW lasing at 1937 nm was reached from a piece of 40-cm long, purposely developed highly Tm-doped tungsten-tellurite glass double cladding fiber [35]. The pumped end of the fiber was coated with a dichroic thin film with high reflectivity near 1950 nm and antireflective near 800 nm. This dielectric coating served as a high-reflection mirror of the fiber laser cavity. Fresnel reflection of approximately 13% from the other cleaved end of the tellurite glass fiber functioned as a

Peer-reviewed version available at Fibers 2020, 8, 30; doi:10.3390/fib8050030

partially reflective output mirror of the laser cavity. The slope efficiency and the optical–optical efficiency with respect to the absorbed pump were 20% and 16%, respectively [35].

The first passively Q-switched Tm^{3+}-doped tellurite fiber laser was reported in [38]. Both carbon nanotubes (CNTs) and a semiconductor saturable absorber mirror (SESAM) were inserted separately into the laser cavities as saturable absorbers to demonstrate a fiber integrated setup. In a piece of 9-cm long tellurite fiber, pulsed lasing at 1.86 μm without self-mode-locking effect was observed with in-band pumping at 1.59 μm. An average power of 84 mW was obtained in a CNT Q-switched laser with 860 ns pulse duration while in a SESAM Q-switched laser, the average power of 21 mW for 516 ns pulse duration was attained. Pulse energies were 736 nJ and 193 nJ for CNT- and SESAM-based configuration, respectively [38].

The transition from supercontinuum generation to 1.887 μm CW lasing in a Tm-doped tellurite microstrucured fiber pumped by a femtosecond fiber laser system at 1.56 μm was observed in [37] for the first time. This transition occurred when varying pulse duration of the pump laser from 0.29 to 3.47 ps. The microstructured 20-cm long fiber made of Tm-doped $78TeO_2$-$5ZnO$-$12Na_2CO_3$-$5Bi_2O_3$ glass had a "wagon wheel" cross-section with a solid core surrounded by six air holes. With a decrease in the pump pulse duration from 3.4 ps to 1.3 ps, the threshold of the 1.887 μm laser decreased monotonically from 232 mW to 216 mW and the corresponding slope efficiency increased from 10.2% to 14.8% [37].

4.2. Lasing near 2.3 μm in Tm-doped fibers

Achieving laser generation at the $^3H_4 \rightarrow {}^3H_5$ transition near 2.3 μm is a more complicated problem than at the $^3F_4 \rightarrow {}^3H_6$ transition in the 1.9-2 μm range, since the lifetime of the $^3H_4$ level is an order of magnitude shorter than the lifetime of the $^3F_4$ level (~0.3 ms against ~3 ms [74]), and the maximum emission cross-section of the $^3H_4 \rightarrow {}^3H_5$ transition is smaller than the maximum emission cross-section of the $^3F_4 \rightarrow {}^3H_6$ transition [74]. Therefore, when producing new tellurite glass fibers for generation at 2.3 μm, more stringent conditions should be imposed on the quality of the samples in comparison with the samples for generation only in the 1.9-2 μm spectral range. It is desirable to fabricate a high-quality low loss fiber, with a very low content of OH^- groups. In addition, the concentration of Tm^{3+} ions should be selected carefully. On the one hand, high concentrations lead to shorter pump absorption lengths, consequently, to less impact of losses. On the other hand, at a high concentration, the cross-relaxation process ($^3H_4 + {}^3H_6 \rightarrow {}^3F_4 + {}^3F_4$) becomes significant and contributes to depopulation of the energy level $^3H_4$. Note that for laser generation at the $^3F_4 \rightarrow {}^3H_6$ energy transition, cross relaxation is a helpful process, but for generation at the $^3H_4 \rightarrow {}^3H_5$ transition it is parasitic. Therefore, for generating in the ~2.3 μm spectral range, special attention should be paid to the parameters of glass. As in the case of generation at ~2.7 μm in Er-doped fibers ("the third opportunity"), the bottleneck problem in Tm-doped fibers with a short lifetime of the upper energy level $^3H_4$ compared with the underlying level $^3F_4$ can be solved by cascade lasing at two transitions $^3H_4 \rightarrow {}^3H_5$ and $^3F_4 \rightarrow {}^3H_6$. The first experimental demonstration of two-color CW lasing simultaneously near 1.9 μm and 2.3 μm in the tellurite TeO_2-ZnO-La_2O_3-Na_2O glass fiber with Tm-doped core having a concentration of $5 \cdot 10^{19}$ cm^{-3} was reported in [11]. A theoretical investigation of laser amplification and generation, which is in a very good agreement with the experimental results, was also performed in [11]. A quantitatively verified numerical model was used to predict power scalability at 2.3 μm in two-color cascade schemes with optimized parameters under increased pump power. It was simulated that the maximum output power at 2.3 μm can exceed 0.6 W for backward 10-W pump. Using the same fiber, experimental ultrabroadband amplification of supercontinuum was also obtained with maximum gain of 30 dB and 7 dB at 1.9 μm and 2.3 μm, respectively [11].

The specific problem of short lifetime of the upper laser level for generation at ~2.3 μm can be also solved by using pulsed pump (analogously to "the second way" of lasing in the 2.7-2.8 μm region in Er-doped fibers). This path to generate laser pulses at 2.3 μm in Tm-doped TeO_2-ZnO-La_2O_3-Na_2O glass fiber under diode pulsed pump at 794 nm was experimentally realized in [12] by setting 1 ms pump duration and 10 ms interval between pulses.

Peer-reviewed version available at Fibers 2020, 8, 30; doi:10.3390/fib8050030

Tm-doped tellurite glass elements can be also used as gain media in the S-band near 1.47-1.48 μm at the $^3H_4 \rightarrow {}^3F_4$ transition. The possibility of amplification was demonstrated in several papers including under single wavelength pumping at ~795 nm [75] as well as under dual-wavelength pumping at 795 nm and 1064 nm [75,76], at 1550 nm and at 1047 nm [76], at 1047 nm and at 1605 nm [77], but laser generation at the $^3H_4 \rightarrow {}^3F_4$ transition in a Tm-doped tellurite fiber has not been reported yet.

4.3. Lasing in Tm-doped microspheres

Tm-doped tellurite microsphere lasers generating only at the $^3F_4 \rightarrow {}^3H_6$ transition near 1.9 μm as well as at two consecutive transitions $^3H_4 \rightarrow {}^3F_4$ and $^3F_4 \rightarrow {}^3H_6$ simultaneously near 1.5 and 1.9 μm in the cascade scheme were reported in [41-46]. Note that such a cascade two-color generation scheme was not implemented for tellurite fiber lasers.

The first Tm-doped tellurite microsphere laser was presented in 2004 [41] by the same research team that constructed the first Nd-doped tellurite microsphere laser [17]. The Tm-doped tellurite microsphere was fabricated by melting the end of a tellurite glass wire, and the microlaser was pumped at 800 nm using a tapered optical fiber. Generation was observed simultaneously in the *S*-band and in the 1.9 μm band. The threshold in the 1.9 μm band was lower than in the *S*-band, and the quantum efficiency in the 1.9 μm band increased with pump power above the lasing threshold of the *S*-band [41].

A single-mode microlaser at 2 μm pumped by a 973 nm Ti:sapphire laser was demonstrated from a highly Tm-doped tellurite glass microsphere with a diameter of 25 μm [42]. Fiber taper was used for pump coupling and laser signal outputting. Note that in the theoretical study of 2-μm lasing in Tm-doped microspheres presented in [57], the obtained numerical results agreed with the experimental ones [42].

A Tm/Ho co-doped tellurite glass microsphere laser at ~1.47 μm was implemented at the $^3H_4 \rightarrow {}^3F_4$ energy transition of the Tm^{3+} ion [46]. Ho^{3+} was co-doped to Tm^{3+} to reduce the population of the long-lived $^3F_4$ state of the Tm^{3+} ion through a resonant energy transfer process. Using a CO_2 laser, microspheres with diameters ranging from several micrometers to several hundred micrometers were produced. Both ~802 nm pump light of a laser diode and the lasing emission were efficiently guided through a silica tapered fiber. Multimode lasing near 1.47 μm as well as single-mode lasing at 1494.9 nm were demonstrated [46].

Recently, 1.9 μm laser generation and visible light of green and red emissions in Er/Tm co-doped tellurite glass microspheres were reached at pumping by 1550 nm broadband amplified spontaneous emission source [45]. Adjusting the coupling position between the microsphere and the tapered optical fiber, a microlaser with single-mode performance was obtained. The output power was 0.21 μW at 1891.63 nm, the side-mode suppression ratio was 12.04 dB, and the line width was 0.18 nm. The threshold power coupled into a microsphere was 1.5 mW. Single-mode and multimode lasing was observed by adjusting the coupling [45].

A theoretical investigation of multi-color CW lasing in Tm-doped tellurite glass microspheres pumped at a wavelength near 0.8 μm was presented in [58]. The numerical model was based on solving a system of equations for intracavity field amplitudes for all fundamental WGMs in the gain bands and rate equations using experimental parameters of Tm-doped tellurite glass. It was shown that, depending on Q-factors and pump powers, different generation regimes can be attained including single-color lasing at a wavelength of ~1.9 μm, two-color lasing at wavelengths of ~1.9&1.5 μm and at ~1.9&2.3 μm, and three-color lasing at wavelengths of ~1.9&1.5&2.3 μm [58]. But unlike fiber lasers generated at 2.3 μm [11,12], tellurite microlasers at 2.3 μm have not yet been reported. The theoretical results obtained in [58] agreed with the experimental data reported in [41,43].

5. Holmium

Generation in the 2-2.1 μm range can be attained with Ho^{3+} ion at the $^5I_7 \rightarrow {}^5I_8$ transition, which is shown in Fig. 7. But unlike Nd^{3+}, Er^{3+}, and Tm^{3+} ions considered above, Ho^{3+} has no absorption bands corresponding to commercial low cost laser diodes at wavelength of ~800 nm or ~980 nm. In-band

Peer-reviewed version available at Fibers 2020, 8, 30; doi:10.3390/fib8050030

pumping at the $^5I_8 \rightarrow {}^5I_7$ transition can be implemented by Tm-doped silica fiber lasers. Pumping at the $^5I_8 \rightarrow {}^5I_6$ transition near 1.1 μm by a specially designed fiber laser, including Raman lasers can be also reasonable. Another way is to use co-doping with a sensitising ion to provide useful absorption bands. A popular ion for co-doping is Tm^{3+} pumped near 800 nm by a laser diode. In this case, a two-for-one cross-relaxation process can be exploited, and the energy transfer from the $^3F_4$ level of the Tm^{3+} ion to the $^5I_7$ level of the Ho^{3+} ion can be very efficient. Co-doping with Yb^{3+} ions allows pumping by laser diodes at 980 nm. Nd^{3+} ions can be also used as sensitiser, which was recently proposed and demonstrated for a 795-nm diode pumped Nd/Ho co-doped tellurite fiber laser [51].

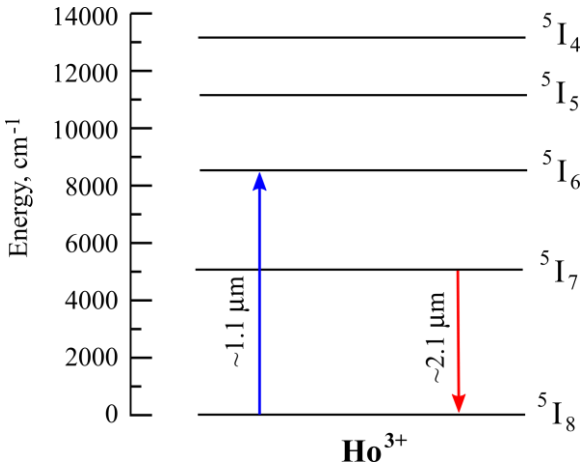

Figure 7. Simplified energy level diagram for Ho-doped tellurite glass.

5.1. Lasing in Ho-doped fibers

CW lasing at 2.1 μm from a Yb/Tm/Ho triply-doped tellurite fiber laser was reported in [48]. The generation at the $^5I_7 \rightarrow {}^5I_8$ transition of Ho^{3+} ions was observed. Using an Yb-doped double-clad silica fiber laser at 1.1 μm as a pump source, it was suggested to co-dope tellurite gain fiber for sensitisation by both Yb^{3+} and Tm^{3+} ions to provide a more efficient energy transfer route than sensitization by Yb^{3+} alone. For a 17 cm fiber length and 99%–60% reflectance cavity, the threshold was 15 mW and the slope efficiency was 25%. A maximum output of 60 mW was observed for a launched pump power of 270 mW corresponding to 22% optical-to-optical efficiency. The same authors reported CW and Q-switch lasing from a Tm/Ho/Yb co-doped tellurite fiber pumped at ~1.6 μm by an Er/Yb silica fiber laser (the Yb^{3+} ions were added with other experiments in mind; they have no absorption at wavelengths >1.1 μm and therefore were not thought to play an active role) [48]. For CW operation, the slope efficiency was 62% and the threshold was 0.1 W; the maximum output power was 0.16 W. Mechanical *Q*-switching resulted in pulses with an energy of 0.65 μJ and a pulse duration of 160 ns at a repetition rate of 19.4 kHz was achieved [48].

A watt-level generation at 2051 μm with a slope efficiency of 31.9% was attained with 50-cm long Ho/Tm co-doped $50TeO_2$-$25GeO_2$-$3WO_3$-$5La_2O_3$-$3Nb_2O_5$-$5Li_2O$-$9BaF_2$ glass fiber pumped by an Er-doped fiber laser at 1560 nm [52]. The threshold power was 0.336 W. The maximum output power was 0.993 W when the pump power was 2.97 W [52].

A multiwatt laser output from a 30 cm long Ho-doped fluorotellurite microstructured fiber pumped by a 1980 nm Tm-doped silica fiber laser was recently reported in [53]. When the threshold pump power was 61.8 mW, lasing at 2067 nm started. An unsaturated maximum output power of ~8.08 W was obtained for a pump power of ~10.56 W. The corresponding slope efficiency was about 77%. Numerical simulation of lasing for experimental parameters was also performed by solving the rate equations and propagation equations. The experimental and numerical results were in a good agreement [53].

5.2. Lasing in Ho-doped microspheres

Peer-reviewed version available at Fibers 2020, 8, 30; doi:10.3390/fib8050030

A single-mode Ho-doped tellurite glass microsphere laser directly pumped by a fiber laser at 1150 nm was studied in [55]. The lasing at ~2 μm with a low-threshold of 342 μW was achieved. The dynamic characteristics of the microsphere laser were also studied theoretically by considering rare-earth ion spectroscopy, the rate equation of the rare-earth energy level, and the light-matter interactions in the microsphere [55].

The fabrication and characterization of microsphere lasers operating at wavelengths near 2.1 μm was reported in [54]. A Tm/Ho co-doped tellurite glass was used as the base material and a droplet method was implemented to produce hundreds of high quality microspheres simultaneously (with Q-factors reaching 10^6). Using a laser diode at 808 nm as a pump source, single-mode and multimode generation was obtained as the pump power was increased beyond a threshold of 0.887 mW. The highest laser power reached 105.8 nW and the longest laser wavelength reached 2099.52 nm for a 59.52-μm sphere diameter. It was also demonstrated that a microsphere laser could be thermally tuned with a sensitivity of 32 pm/°C [54].

6. Opportunities for other rare-earth ions

In addition to the rare-earth ions discussed above, using other rare-earth ions for the development of tellurite glass based laser elements was investigated and discussed. There are a lot of works reporting the production of tellurite glass samples doped with Yb^{3+} [78,79], Dy^{3+} [67,80,81], Pr^{3+} [81-83], Eu^{3+} [81,84], Tb^{3+} [81,85], and Sm^{3+} [85,86] and study of their luminescent and other optical, physical and chemical properties. However, we could not find information about laser generation in tellurite glass fibers or microspheres operating at the radiative transitions of these rare-earth ions.

7. Summary

The state of the art of tellurite glass fiber and microsphere lasers has been reviewed. It has been demonstrated that high-quality rare-earth doped tellurite fibers are promising novel gain elements for lasers and amplifiers in the L-band and in the range of 2 μm and well beyond. Tellurite microsphere lasers are also an attractive platform for developing ultracompact, low threshold, narrow linewidth light sources. The main experimental results on tellurite glass fiber lasers and microsphere lasers are summarized in Table 1 and in Table 2, respectively.

Table 1. Summary of performance of rare-earth doped tellurite glass fiber lasers.

Dopant	Glass composition	Fiber length, cm	Pump laser, pump wavelength, nm	CW or pulsed	Laser wavelength, nm	Maximum output power (or energy)	Year, reference
Nd^{3+}	$76.9TeO_2$-$6.0Na_2O$-$15.5ZnO$-$1.5Bi_2O_3$-$0.1Nd_2O_3$	60	Ti: sapphire, 818	CW	1061	4.2 mW	1994 [16]
Er^{3+}	Not reported	85	Ti: sapphire, 978	CW	1560	2.5 mW	1997 [22]
Er^{3+}, $0.9{\cdot}10^{20}$ cm^{-3}, Ce^{3+}, $2.1{\cdot}10^{20}$ cm^{-3}	$80TeO_2$-$10ZnO$-$10Na_2O$	22	Laser diodes, 980&1480	CW	1527-1610	0 dBm (1 mW) @1558 nm	2011 [23]

Peer-reviewed version available at Fibers 2020, 8, 30; doi:10.3390/fib8050030

Er^{3+}, $8.12 \cdot 10^{19}$ cm^{-3}, Ce^{3+}, $1.92 \cdot 10^{19}$ cm^{-3}	$79TeO_2$-$13ZnO$-$8Na_2O$	10	Laser diodes, 980&1480	CW	~1550	2.6 mW	2012 [24]
Er^{3+}, 10^{19} cm^{-3}	TeO_2-ZnO-La_2O_3-Na_2O	~220	Laser diode, 974	CW	~1550	<1 mW	2012 [25]
Er^{3+} , (7500 ppm Er_2O_3)	$71TeO_2$-$22.5WO_3$-$5Na_2O$-$1.5Nb_2O_5$	5-16	Laser diode, 980	CW	1530-1565	≤ -24.39 dBm (≤3.6 μW)	2012 [26]
Er^{3+}, (Er_2O_3 5000 ppm)	$78TeO_2$-$5ZnO$-$12Na_2CO_3$-$5Bi_2O_3$	17	Laser diode, 1480	CW	1561	140 mW	2013 [27]
Er^{3+}, 10000 ppm	$76.5TeO_2$-$6Bi_2O_3$-$6ZnO$-$11.5Li_2O$	14	Fiber Raman laser, 1480	Pulsed (self-Q-switch)	1558	316 mW	2014 [28]
Er^{3+}, 10^{20} cm^{-3}	TeO_2-ZnO-La_2O_3-Na_2O	20	Laser diode, 975	CW	1555	>100 μW	2019 [29]
Er^{3+}, 1wt.%	(50-80) TeO_2-(10-40) ZnO-(10-x) La_2O_3-xEr_2O_3	~300	Fiber laser, 1570	CW	1589-1627	52.4 mW @ 1614 nm	2019 [30]
Tm^{3+}/ Yb^{3+} (1.5/1.0 wt% Yb_2O_3/ Tm_2O_3)	$80TeO_2$-$10ZnO$-$10Na_2O$	32	Fiber laser, 1568-1610	CW	1880-1990	280 mW	2008 [33]
Tm^{3+}/ Yb^{3+} (1.5/1.0 wt% Yb_2O_3/ Tm_2O_3)	$80TeO_2$-$10ZnO$-$10Na_2O$	22	Fiber laser, 1088	CW	1910-1994	67 mW	2009 [34]
Tm^{3+} $3.76 \cdot 10^{20}$ cm^{-3}	$60TeO_2$-$30WO_3$-$10La_2O_3$	40	Laser diode, 800	CW	1937	1.12 W	2010 [35]
Tm^{3+}, 1mol.%	$60TeO_2$-$30WO_3$-$10La_2O_3$	20	Laser diode, 793	CW	~1900	494 mW	2012 [36]
Tm^{3+}, 5000 ppm	$78TeO_2$-$5ZnO$-	20	Femto-second	CW	1887	>6.5 mW	2014 [37]

Peer-reviewed version available at Fibers 2020, 8, 30; doi:10.3390/fib8050030

	$12Na_2CO_3$-$5Bi_2O_3$		fiber system, 1560				
Tm^{3+}, $3.76 \cdot 10^{20}$ cm^{-3}	Not reported	9	Fiber laser, 1590	Pulsed (Q-switch)	1860	84 mW, 736 nJ	2015 [38]
Tm^{3+}, 1mol.% Tm_2O_3	$45GeO_2$-$25TeO_2$-15PbO-10(La_2O_3 +Al_2O_3)-5(CaO+ SrO+ Li_2O)	26	Laser diode, 793	CW	1968	0.75 W	2015 [39]
Tm^{3+}, 0.5% Tm_2O_3	$70TeO_2$-$10BaF_2$-$9.5Y_2O_3$-$0.5Tm_2O_3$	42.5	Fiber laser, 1570	CW	1887	408 mW	2017 [40]
Tm^{3+}, $5 \cdot 10^{19}$ cm^{-3}	TeO_2-ZnO-La_2O_3-Na_2O	~220	Laser diode, 792	CW	2300& 1950	1.7 mW @2300 nm, ~40 mW @1950 nm	2018 [11]
Tm^{3+}, $5 \cdot 10^{19}$ cm^{-3}	(86−*x*) TeO_2-*x*ZnO-$4La_2O_3$-$10Na_2O$	30	Laser diode, 794	Pulsed	2300; 2300& 1900	A few μW	2019 [12]
Tm^{3+}/ Ho^{3+}/ Yb^{3+}, (1.5/ 1.0/ 1.0 wt% Yb_2O_3/ Tm_2O_3/ Ho_2O_3)	$80TeO_2$–10ZnO–$10Na_2O$	17	Fiber laser, 1088	CW	~2100	60 mW	2008 [47]
Tm^{3+}/ Ho^{3+}/ Yb^{3+}, (1.5/ 1.0/ 1.0 wt% Yb_2O_3/ Tm_2O_3/ Ho_2O_3)	$80TeO_2$–10ZnO–$10Na_2O$	76	Fiber laser, 1600	CW	2051-2096	160 mW	2008 [48]
		79	Fiber laser, 1600	Pulsed (Q-switch)	~2100	26 mW, 1.3 μJ (train), 0.65 μJ (main pulse)	
Tm^{3+}/ Ho^{3+}, 1mol%/ 0.5mol%	$60TeO_2$-$30WO_3$-$10La_2O_3$	7	Laser diode, 793	CW	2046	35 mW	2012 [36]
Ho^{3+}, 0.75% Ho_2O_3	$70TeO_2$–$20BaF_2$–$9.25Y_2O_3$–	27	Fiber laser, 1992	CW	2077	161 mW	2015 [49]

Peer-reviewed version available at Fibers 2020, 8, 30; doi:10.3390/fib8050030

	$0.75Ho_2O_3$						
Ho^{3+}, 0.5% Ho_2O_3	$60TeO_2$–$30WO_3$–$9.5La_2O_3$–$0.5Ho_2O_3$	9	Fiber laser, 1940	CW	2040	34 mW	2016 [50]
Nd^{3+}/ Ho^{3+}, 0.5% Nd_2O_3/ 0.5% Ho_2O_3	$60TeO_2$–$30WO_3$–$3ZnO$–$6La_2O_3$–$0.5Ho_2O_3$–$0.5Nd_2O_3$	5	Laser diode, 975	CW	2052	12 mW	2016 [51]
Tm^{3+}/Ho^{3+}, Ho_2O_3: 0.3%mol, Tm_2O_3: 0.3%mol	$50TeO_2$-$25GeO_2$-$3WO_3$-$5La_2O_3$-$3Nb_2O_5$-$5Li_2O$-$9BaF_2$	50	Fiber laser, 1560	CW	2051	0.993	2017 [52]
Ho^{3+}, 0.75% Ho_2O_3	$70TeO_2$-$20BaF_2$-$9.25Y_2O_3$-$0.75Ho_2O_3$	30	Fiber laser, 1980	CW	2067	8.08 W	2019 [53]

Peer-reviewed version available at Fibers 2020, 8, 30; doi:10.3390/fib8050030

Table 2. Summary of performance of rare-earth doped tellurite glass microsphere lasers.

Dopant	Glass composition	Sphere diameter, μm	Pump laser, pump wavelength, nm	Single-mode (SM) or multi-mode (MM)	Laser wavelength, nm	Year, reference
Nd^{3+}, (1wt% Nd_2O_3)	$70TeO_2$-20ZnO-$10Li_2O$	201 (50- a few hundred)	Ti: sapphire, 800	MM	~1060 (1061-1067)	2002 [17]
Nd^{3+}, (0.2 wt% Nd_2O_3)	$75TeO_2$-20ZnO-$5Na_2O$	~70-180	Ti: sapphire, 800	SM and MM	~1058-1075	2003 [18]
Nd^{3+}, (1mol% Nd_2O_3)	$80TeO_2$-$10K_2O$-$10WO_3$ air-bubble-containing or solid	~20-50	Ti: sapphire, 810	MM	~1060-1070	2012 [19]
Nd^{3+}, (1mol% Nd_2O_3)	$80TeO_2$-$10K_2O$-$10WO_3$	29	Ti: sapphire, 800-810	SM and MM	~1060-1070	2015 [20]
Nd^{3+}, (1mol% Nd_2O_3)	$80TeO_2$-$10K_2O$-$10WO_3$ air-bubble-containing or solid	~4-200	Ti: sapphire, 790–817	MM	~1060-1070	2015 [21]
Er^{3+}, ($1.7 \cdot 10^{20}$ cm^{-3})	Not reported	33	975	SM and MM	1560-1610	2003 [31]
Er^{3+}	Not reported	31	1480	SM	~1606-1608	2003 [32]
Tm^{3+}, (0.15% Tm_2O_3)	$74.85TeO_2$-20ZnO-$5Na_2O$-$0.15Tm_2O_3$	104	Ti: sapphire, 800	MM	~1500& 1900	2004 [41]
Tm^{3+}, (5wt%)	Not reported	25	Ti: sapphire, 793	SM	~2000	2005 [42]
Tm^{3+}, 0.5wt% Tm_2O_3	Not reported	Not reported	Ti: sapphire, 793	MM	~1500& 1900	2005 [43]
Tm^{3+}, ($4.2 \cdot 10^{20}$ cm^{-3})	$74TeO_2$-15ZnO-$5Na_2O$-$5ZnCl_2$-$1Tm_2O_3$ (mol. %)	30	1504-1629	MM	Centered at ~1975	2015 [44]
Er^{3+}/Tm^{3+} (0.1/0.2% Er_2O_3/	$68.7TeO_2$-$23WO_3$-$8La_2O_3$-	110	Amplified sponta-neous	SM and MM	~1900	2019 [45]

Peer-reviewed version available at Fibers 2020, 8, 30; doi:10.3390/fib8050030

Tm_2O_3)	0.1Er_2O_3-0.2Tm_2O_3 (mol%)		emission source, 1527-1603			
Tm^{3+}/Ho^{3+} (0.2/0.8% Tm_2O_3/ Ho_2O_3)	72TeO_2-20ZnO-5.0Na_2CO_3-2.0Y_2O_3-0.8Ho_2O_3-0.2Tm_2O_3	~100	Laser diode, 802	SM and MM	~1470	2019 [46]
Tm^{3+}/Ho^{3+} (1.0/0.7% Tm_2O_3/ Ho_2O_3)	75TeO_2-18.3ZnO-5Na_2O-1.0Tm_2O_3-0.7Ho_2O_3	~60	Laser diode, 808	SM and MM	~2100	2017 [54]
Ho^{3+}, (1mol% HoF_3)	72TeO_2-20ZnO-5Na_2CO_3-2Y_2O_3-1HoF_3 (in mol%)	~42	Fiber laser, 1150	SM	~2080	2020 [55]
Ho^{3+}/Yb^{3+} (0.2/0.8% Ho_2O_3/ Yb_2O_3)	72TeO_2-20ZnO-5Na_2CO_3-2Y_2O_3-0.8Yb_2O_3-0.2Ho_2O_3	80	Laser diode, 980	SM and MM	~2065-2072	2020 [56]

Funding: The review of microsphere lasers was funded by the Russian Science Foundation, grant no. 18-72-00176. The review of fiber lasers was funded by the Russian Foundation for Basic Research, grant number 20-03-00874.

Conflicts of Interest: The author declares no conflict of interest.

References

1. El-Mallawany, R.A.H. *Tellurite Glasses Handbook: Physical Properties and Data*. CRC press, 2016.
2. Rivera, V.A.G., Manzani, D. Eds. *Technological Advances in Tellurite Glasses*. Springer Series in Materials Science, 2017; Volume 254. https://doi.org/10.1007/978-3-319-53038-3
3. Tao, G., Ebendorff-Heidepriem, H., Stolyarov, A. M., Danto, S., Badding, J. V., Fink, Y., Ballato, J., Abouraddy, A. F. Infrared fibers. *Advances in Optics and Photonics* **2015**, 7, 379-458. https://doi.org/10.1364/AOP.7.000379
4. Jha, A., Richards, B., Jose, G., Teddy-Fernandez, T., Joshi, P., Jiang, X., Lousteau, J. Rare-earth ion doped TeO_2 and GeO_2 glasses as laser materials. *Prog. Mater. Sci.* **2012**, 57, 1426-1491. http://dx.doi.org/10.1016/j.pmatsci.2012.04.003
5. Smayev, M. P., Dorofeev, V. V., Moiseev, A. N., Okhrimchuk, A. G. Femtosecond laser writing of a depressed cladding single mode channel waveguide in high-purity tellurite glass. *Journal of Non-crystalline Solids* **2018**, 480, 100-106. https://doi.org/10.1016/j.jnoncrysol.2017.11.007
6. Yakovlev, A. I., Snetkov, I. L., Dorofeev, V. V., Motorin, S. E. Magneto-optical properties of high-purity zinc-tellurite glasses. *Journal of Non-Crystalline Solids* **2018**, 480, 90-94. https://doi.org/10.1016/j.jnoncrysol.2017.08.026
7. Alazoumi, S. H., Aziz, S. A., El-Mallawany, R., Aliyu, U. S., Kamari, H. M., Zaid, M. H. M. M., Matori, K.A., Ushah, A. Optical properties of zinc lead tellurite glasses. *Results in Physics* **2018**, 9, 1371-1376. https://doi.org/10.1016/j.rinp.2018.04.041

Peer-reviewed version available at Fibers 2020, 8, 30; doi:10.3390/fib8050030

8. Anashkina, E.A., Dorofeev, V.V., Koltashev, V.V., Kim, A.V. Development of Er^{3+}-doped high-purity tellurite glass fibers for gain-switched laser operation at 2.7 μm. *Opt. Mater. Express* **2017**, 7, 4337-4351. https://doi.org/10.1364/OME.7.004337
9. Dorofeev, V. V., Moiseev, A. N., Churbanov, M. F., Kotereva, T. V., Chilyasov, A. V., Kraev, I. A., Pimenov, V.G., Ketkova, L.A., Dianov E.M., Plotnichenko, V.G., Kosolapov, A.F, Kosolapov, A. F. Production and properties of high purity TeO_2–WO_3–(La_2O_3, Bi_2O_3) and TeO_2–ZnO–Na_2O– Bi_2O_3 glasses. *Journal of non-crystalline solids* **2011**, 357, 2366-2370. http://dx.doi.org/10.1016/j.jnoncrysol.2011.01.022
10. Richards, B. D., Jha, A. Lasers utilising tellurite glass-based gain media. In *Technological Advances in Tellurite Glasses*; Rivera, V.A.G., Manzani, D. Eds.; Springer Series in Materials Science, 2017; Volume 254, pp. 101-130. https://doi.org/10.1007/978-3-319-53038-3_6
11. Muravyev, S. V., Anashkina, E. A., Andrianov, A. V., Dorofeev, V. V., Motorin, S. E., Koptev, M. Y., Kim, A. V. (2018). Dual-band Tm^{3+}-doped tellurite fiber amplifier and laser at 1.9 μm and 2.3 μm. *Sci. Rep.* **2018**, 8, 16164. https://doi.org/10.1038/s41598-018-34546-w
12. Denker, B. I., Dorofeev, V. V., Galagan, B. I., Koltashev, V. V., Motorin, S. E., Plotnichenko, V. G., Sverchkov, S. E. 2.3 μm laser action in Tm^{3+}-doped tellurite glass fiber, *Laser Phys. Lett*. **2019**, 16, 015101. https://doi.org/10.1088/1612-202X/aaeda4
13. Reynolds, T., Riesen, N., Meldrum, A., Fan, X., Hall, J. M., Monro, T. M., François, A. Fluorescent and lasing whispering gallery mode microresonators for sensing applications. *Laser Photonics Rev.* **2017**, 11, 1600265. https://doi.org/10.1002/lpor.201600265
14. He, L., Özdemir, Ş. K., Yang, L. Whispering gallery microcavity lasers. *Laser Photonics Rev.* **2012**, 7, 60-82. https://doi.org/10.1002/lpor.201100032
15. Strekalov, D. V., Marquardt, C., Matsko, A. B., Schwefel, H. G., Leuchs, G. Nonlinear and quantum optics with whispering gallery resonators. *Journal of Optics* **2016**, 18, 123002. https://doi.org/10.1088/2040-8978/18/12/123002
16. Wang, J. S., Machewirth, D. P., Wu, F., Snitzer, E., Vogel, E. M. Neodymium-doped tellurite single-mode fiber laser. *Opt. Lett.*, **1994**, 19, 1448-1449. https://doi.org/10.1364/OL.19.001448
17. Sasagawa, K., Kusawake, K., Ohta, J., Nunoshita, M. Nd-doped tellurite glass microsphere laser. *Electron. Lett.* **2002**, 38, 1355-1357. https://doi.org/10.1049/el:20020929
18. Sasagawa, K., Yonezawa, Z., Ohta, J., Nunoshita, M. Control of microsphere lasing wavelength using λ/4-shifted distributed feedback resonator. *Electron. Lett.* **2003**, 39, 1817 – 1819. https://doi.org/10.1049/el:20031156
19. Kishi, T., Kumagai, T., Yano, T., Shibata, S. On-chip fabrication of air-bubble-containing Nd^{3+}-doped tellurite glass microsphere for laser emission. *AIP Advances* **2012**, 2, 042169. https://doi.org/10.1063/1.4769888
20. Kishi, T., Kumagai, T., Shibuya, S., Prudenzano, F., Yano, T., Shibata, S. Quasi-single mode laser output from a terrace structure added on a Nd 3+-doped tellurite-glass microsphere prepared using localized laser heating. *Opt. Express* **2015**, 23, 20629-20635. https://doi.org/10.1364/OE.23.020629
21. Kumagai, T., Kishi, T., Yano, T. Low threshold lasing of bubble-containing glass microspheres by non-whispering gallery mode excitation over a wide wavelength range. *J. Appl. Phys*. **2015**, 117, 113104. https://doi.org/10.1063/1.4915901
22. Mori, A., Ohishi, Y., Sudo, S. Erbium-doped tellurite glass fibre laser and amplifier. *Electron. Lett.* **1997**, 33, 863-864. https://doi.org/10.1049/el:19970585
23. Dong, J., Wei, Y. Q., Wonfor, A., Penty, R. V., White, I. H., Lousteau, J., Jose, G., Jha, A. Dual-Pumped Tellurite Fiber Amplifier and Tunable Laser Using Er^{3+}/Ce^{3+} Codoping Scheme. *IEEE Photonics Technol. Lett*. **2011**, 23, 736-738. https://doi.org/10.1109/LPT.2011.2128864
24. Lousteau, J., Boetti, N. G., Chiasera, A., Ferrari, M., Abrate, S., Scarciglia, G., Venturello, A., Milanese, D. Er^{3+} and Ce^{3+} Codoped Tellurite Optical Fiber for Lasers and Amplifiers in the Near-Infrared Wavelength Region: Fabrication, Optical Characterization, and Prospects. *IEEE Photonics Journal* **2012**, 4, 194-204. https://doi.org/10.1109/JPHOT.2011.2181974
25. Oermann, M. R., Ebendorff-Heidepriem, H., Ottaway, D. J., Lancaster, D. G., Veitch, P. J., Monro, T. M. Extruded microstructured fiber lasers. *IEEE Photonics Technol. Lett.* **2012**, 24, 578-580. https://doi.org/10.1109/LPT.2012.2183863
26. Chillcce, E. F., Narro-García, R., Menezes, J. W., Rodriguez, E., Marconi, D., Fragnito, H. L., Barbosa, L. C. Er^{3+}-doped micro-structured tellurite fiber: laser generation and optical gain. In *Optical Components and*

Peer-reviewed version available at Fibers 2020, 8, 30; doi:10.3390/fib8050030

Materials IX (Vol. 8257, p. 82570B). International Society for Optics and Photonics **2012**. https://doi.org/10.1117/12.909026

27. Jia, Z., Li, H., Meng, X., Liu, L., Qin, G., Qin, W. Broadband amplification and highly efficient lasing in erbium-doped tellurite microstructured fibers. *Opt. Lett.* **2013**, 38, 1049-1051. https://doi.org/10.1364/OL.38.001049
28. Jia, Z. X., Yao, C. F., Kang, Z., Qin, G. S., Ohishi, Y., Qin, W. P. Self-Q-switching behavior of erbium-doped tellurite microstructured fiber lasers. *J. Appl. Phys*. **2014**, 115, 223103. https://doi.org/10.1063/1.4883242
29. Anashkina, E. A., Andrianov, A. V., Dorofeev, V. V., Kim, A. V., Koltashev, V. V., Leuchs, G., Motorin, S.E., Muravyev, S.V., Plekhovich, A. D. Development of infrared fiber lasers at 1555 nm and at 2800 nm based on Er-doped zinc-tellurite glass fiber. *Journal of Non-Crystalline Solids* **2019**, 525, 119667. https://doi.org/10.1016/j.jnoncrysol.2019.119667
30. Fu, S., Zhu, X., Wang, J., Wu, J., Tong, M., Zong, J., Li, M., Wiersma, K., Chavez-Pirson, A., Peyghambarian, N. L-band wavelength-tunable Er^{3+}-doped tellurite fiber lasers. *J. Light. Technol.* **2020**, 38. https://doi.org/10.1109/JLT.2019.2955314
31. Peng, X., Song, F., Jiang, S., Peyghambarian, N., Kuwata-Gonokami, M., Xu, L. Fiber-taper-coupled L-band Er^{3+}-doped tellurite glass microsphere laser. *Appl. Phys. Lett* **2003**, 82, 1497-1499. https://doi.org/10.1063/1.1559653
32. Peng, X., Song, F., Kuwata-Gonokami, M., Jiang, S., Peyghambarian, N. Temperature dependence of the wavelength and threshold of fiber-taper-coupled L-band Er^{3+}-doped tellurite glass microsphere laser. *Appl. Phys. Lett.* **2003**, 83, 5380-5382. https://doi.org/10.1063/1.1637454
33. Richards, B., Tsang, Y., Binks, D., Lousteau, J., Jha, A. Efficient~ 2 μm Tm^{3+}-doped tellurite fiber laser. *Opt. Lett.* **2008**, 33, 402-404. https://doi.org/10.1364/OL.33.000402.
34. Richards, B., Tsang, Y., Binks, D., Lousteau, J., Jha, A. ~ 2 μm Tm^{3+}/Yb^{3+}-doped tellurite fibre laser. *Journal of Materials Science: Materials in Electronics* **2009**, 20, 317-320. https://doi.org/10.1007/s10854-008-9598-0
35. Li, K., Zhang, G., Hu, L. Watt-level~ 2μm laser output in Tm^{3+}-doped tungsten tellurite glass double-cladding fiber. *Opt. Lett.* **2010**, 35, 4136-4138. https://doi.org/10.1364/OL.35.004136
36. Li, K., Zhang, G., Wang, X., Hu, L., Kuan, P., Chen, D., Wang, M. Tm^{3+} and Tm^{3+}-Ho^{3+} co-doped tungsten tellurite glass single mode fiber laser. *Opt. Express* **2012**, 20, 10115-10121. https://doi.org/10.1364/OE.20.010115
37. Jia, Z. X., Liu, L., Yao, C. F., Qin, G. S., Ohishi, Y., Qin, W. P. Supercontinuum generation and lasing in thulium doped tellurite microstructured fibers. *J. Appl. Phys.* **2014**, 115, 063106. https://doi.org/10.1063/1.4865507
38. Kuan, P. W., Li, K., Zhang, L., Fan, X., Hasan, T., Wang, F., Hu, L. All-Fiber Passively Q-Switched Laser Based on Tm^{3+}-Doped Tellurite Fiber. *IEEE Photonics Technol. Lett*. **2015**, 27, 689-692. https://doi.org/10.1109/LPT.2014.2385812
39. Gao, S., Kuan, P. W., Liu, X., Chen, D., Liao, M., Hu, L. ~2 μm Single-Mode Laser Output in Tm^{3+}-Doped Tellurium Germanate Double-Cladding Fiber. *IEEE Photonics Technol. Lett*. **2015**, 27, 1702-1704. https://doi.org/10.1109/LPT.2015.2438077
40. Wang, S., Yao, C., Jia, Z., Qin, G., Qin, W. 1887 nm lasing in Tm^{3+}-doped TeO_2-BaF_2-Y_2O_3 glass microstructured fibers. *Opt. Mater*. **2017**, 66, 640-643. https://doi.org/10.1016/j.optmat.2017.03.019
41. Sasagawa, K., Yonezawa, Z. O., Iwai, R., Ohta, J., Nunoshita, M. S-band Tm 3+-doped tellurite glass microsphere laser via a cascade process. *Appl. Phys. Lett.* **2004**, 85, 4325-4327. https://doi.org/10.1063/1.1810628
42. Wu, J., Jiang, S., Qua, T., Kuwata-Gonokami, M., Peyghambarian, N. 2 μm lasing from highly thulium doped tellurite glass microsphere. *Appl. Phys. Lett.* **2005**, 87, 211118. https://doi.org/10.1063/1.2132532
43. Wu, J., Jiang, S., Peyghambarian, N. 1.5-μm-band thulium-doped microsphere laser originating from self-terminating transition. *Opt. Express* **2005**, 13, 10129-10133. https://doi.org/10.1364/OPEX.13.010129
44. Vanier, F., Côté, F., El Amraoui, M., Messaddeq, Y., Peter, Y. A., Rochette, M. Low-threshold lasing at 1975 nm in thulium-doped tellurite glass microspheres. *Opt. Lett.* **2015**, 40, 5227-5230. https://doi.org/10.1364/OL.40.005227
45. Qin, J., Huang, Y., Liao, T., Xu, C., Ke, C., Duan, Y. 1.9 μm laser and visible light emissions in Er^{3+}/Tm^{3+} co-doped tellurite glass microspheres pumped by a broadband amplified spontaneous emission source. *Journal of Optics* **2019**, 21, 035401. https://doi.org/10.1088/2040-8986/ab0264

Peer-reviewed version available at Fibers 2020, 8, 30; doi:10.3390/fib8050030

46. Li, A., Li, W., Zhang, M., Zhang, Y., Wang, S., Yang, A., Yang, Z., Lewis, E., Brambilla, G., Wang, P. Tm^{3+}-Ho^{3+} codoped tellurite glass microsphere laser in the 1.47 μm wavelength region. *Opt. Lett.* **2019**, 44, 511-513. https://doi.org/10.1364/OL.44.000511
47. Tsang, Y., Richards, B., Binks, D., Lousteau, J., Jha, A. A Yb^{3+}/Tm^{3+}/Ho^{3}+ triply-doped tellurite fibre laser. *Opt. Express* **2008**, 16, 10690-10695. https://doi.org/10.1364/OE.16.010690
48. Tsang, Y., Richards, B., Binks, D., Lousteau, J., Jha, A. Tm^{3+}/Ho^{3+} codoped tellurite fiber laser. *Opt. Lett.* **2008**, 33, 1282-1284. https://doi.org/10.1364/OL.33.001282
49. Yao, C., He, C., Jia, Z., Wang, S., Qin, G., Ohishi, Y., Qin, W. Holmium-doped fluorotellurite microstructured fibers for 2.1 μm lasing. *Opt. Lett.* **2015**, 40, 4695-4698. https://doi.org/10.1364/OL.40.004695
50. Li, D., Xu, W., Kuan, P., Li, W., Lin, Z., Wang, X., Zhang, L., Yu, C., Li., K., Hu, L. Spectroscopic and laser properties of Ho^{3+} doped lanthanum-tungsten-tellurite glass and fiber. *Ceramics International* **2016**, 42, 10493-10497. https://doi.org/10.1016/j.ceramint.2016.03.076
51. Li, L. X., Wang, W. C., Zhang, C. F., Yuan, J., Zhou, B., Zhang, Q. Y. 2.0 μm Nd^{3+}/Ho^{3+}-doped tungsten tellurite fiber laser. *Opt. Mater. Express* **2016**, 6, 2904-2914. https://doi.org/10.1364/OME.6.002904
52. Zhou, D., Bai, X., Zhou, H. Preparation of Ho^{3+}/Tm^{3+} co-doped lanthanum tungsten germanium tellurite glass fiber and its laser performance for 2.0 μm. *Sci. Rep.* **2017**, 7, 44747. https://doi.org/10.1038/srep44747
53. Zhao, Z. P., Yao, C. F., Li, Z. R., Jia, Z. X., Qin, G. S., Ohishi, Y., Qin, W. P. 8.08 W holmium doped fluorotellurite fiber laser at 2067 nm. *Las. Phys. Lett.* **2019**, 16, 115101. https://doi.org/10.1088/1612-202X/ab4599
54. Yang, Z., Wu, Y., Yang, K., Xu, P., Zhang, W., Dai, S., Xu, T. Fabrication and characterization of Tm^{3+}-Ho^{3+} co-doped tellurite glass microsphere lasers operating at ~2.1 μm. *Optical Materials* **2017**, 72, 524-528. https://doi.org/10.1016/j.optmat.2017.06.057
55. Yu, J., Wang, X., Li, W., Zhang, M., Zhang, J., Tian, K., Du, Y., Nic Chormaic, S., Wang, P. An experimental and theoretical investigation of a 2 μm wavelength low-threshold microsphere laser. *Journal of Lightwave Technology* **2020**, 38. https://doi.org/10.1109/JLT.2019.2958349
56. Li, A., Dong, Y., Wang, S., Jia, S., Brambilla, G., Wang, P. Infrared-laser and upconversion luminescence in Ho^{3+}-Yb^{3+} codoped tellurite glass microsphere. *Journal of Luminescence* **2020**, 218, 116826. https://doi.org/10.1016/j.jlumin.2019.116826
57. Saffari, M., Gholami, A., Parsanasab, G.-M., Firouzeh, Z.H. Investigation of a High-Power Low-Threshold Single-Mode Microsphere Laser Using a Serially Coupled Double Microsphere Structure. *Journal of Lightwave Technology* **2019**, 37, 3273-3279. https://doi.org/10.1109/JLT.2019.2913901
58. Anashkina, E.A., Leuchs, G., Andrianov, A.V. Numerical simulation of multi-color laser generation in Tm-doped tellurite microsphere at 1.9, 1.5 and 2.3 microns. *Results in Physics* **2020**, 16, 102811. https://doi.org/10.1016/j.rinp.2019.102811
59. Anashkina, E.A., Andrianov, A.V., Dorofeev, V.V., Muravyev, S.V., Koptev, M.Y., Sorokin, A.A., Motorin, S.E., Koltashev, V.V., Galagan, B.I., Denker, B.I. Two-color pump schemes for Er-doped tellurite fiber lasers and amplifiers at 2.7–2.8 μm. *Las. Phys. Lett.* **2019**, 16, 025107. https://doi.org/10.1088/1612-202X/aaf79a
60. Michel, J. C., Morin, D., uzel, F. Propriétés spectroscopiques et effet laser d'un verre tellurite et d'un verre phosphate fortement dopés en néodyme. *Revue de physique appliquee* **1978**, 13, 859-866. https://doi.org/10.1051/rphysap:019780013012085900
61. Gomes, L., Oermann, M., Ebendorff-Heidepriem, H., Ottaway, D., Monro, T., Felipe Henriques Librantz, A., Jackson, S. D. Energy level decay and excited state absorption processes in erbium-doped tellurite glass. *J. Appl. Phys.* **2011**, 110, 083111. https://doi.org/10.1063/1.3651399
62. Oermann, M. R., Ebendorff-Heidepriem, H., Li, Y., Foo, T. C., Monro, T. M. Index matching between passive and active tellurite glasses for use in microstructured fiber lasers: Erbium doped lanthanum-tellurite glass. *Opt. Eexpress* **2009**, 17, 15578-15584. https://doi.org/10.1364/OE.17.015578
63. Ma, Y., Guo, Y., Huang, F., Hu, L., Zhang, J. Spectroscopic properties in Er^{3+} doped zinc-and tungsten-modified tellurite glasses for 2.7 μm laser materials. *Journal of luminescence* **2014**, 147, 372-377. https://doi.org/10.1016/j.jlumin.2013.11.077
64. Wang, W.C., Yuan, J., Li, L.X., Chen, D.D.,Qian, Q., Zhang, Q.Y. Broadband 2.7 μm amplified spontaneous emission of Er^{3+} doped tellurite fibers for mid-infrared laser applications. *Opt. Mater. Express* **2015**, 5, 2964-2977. https://doi.org/10.1364/OME.5.002964

Peer-reviewed version available at Fibers 2020, 8, 30; doi:10.3390/fib8050030

65. Chen, F., Wei, T., Jing, X., Tian, Y., Zhang, J., Xu, S., Investigation of mid-infrared emission characteristics and energy transfer dynamics in Er^{3+} doped oxyfluoride tellurite glass. *Sci. Rep*. **2015**, 5 10676. https://doi.org/10.1038/srep10676
66. Anashkina, E.A., Dorofeev, V.V., Muravyev, S.V., Motorin, S.E., Andrianov, A.V., Sorokin, A.A., Koptev, M.Yu., Singh, S., Kim, A.V. Possibilities of laser amplification and measurement of the field structure of ultrashort pulses in the range of 2.7 –3 μm in tellurite glass fibres doped with erbium ions. *Quantum Electron*. **2018**, 48, 1118 –1127. https://doi.org/10.1070/QEL16845
67. Denker, B. I., Dorofeev, V. V., Galagan, B. I., Koltashev, V. V., Motorin, S. E., Sverchkov, S. E., Plotnichenko, V. G. Rare-earth ions doped zinc-tellurite glass for 2÷ 3 μm lasers. *Applied Physics B* **2018**, 124, 235. https://doi.org/10.1007/s00340-018-7107-6
68. Aydin, Y.O., Fortin, V., Maes, F., Jobin, F., Jackson, S.D., Vallée, R., Bernier, M. Diode-pumped mid-infrared fiber laser with 50% slope efficiency, *Optica* **2017**, 4, 235-238, https://doi.org/10.1364/OPTICA.4.000235
69. Sujecki, S., Sojka, L., Seddon, A.B., Benson, T.M., Barney, E., Falconi, M.C., Prudenzano, F., Marciniak, M., Baghdasaryan, H., Peterka, P., Taccheo, S. Comparative modeling of infrared fiber lasers. *Photonics* **2018**, 5, 48. https://doi.org/10.3390/photonics5040048
70. Cajzl, J., Peterka, P., Kowalczyk, M., Tarka, J., Sobon, G., Sotor, J., Aubrecht, J., Honzátko, P. and Kašík, I. Thulium-doped silica fibers with enhanced fluorescence lifetime and their application in ultrafast fiber lasers. *Fibers* **2018**, 6, 66. https://doi.org/10.3390/fib6030066
71. Sujecki, S. Modelling and design of lanthanide ion-doped chalcogenide fiber lasers: Progress towards the Practical realization of the first MIR chalcogenide fiber laser. *Fibers* **2018**, 6, 25. https://doi.org/10.3390/fib6020025
72. Anashkina, E.A., Kim, A.V. Numerical simulation of ultrashort mid-IR pulse amplification in praseodymium doped chalcogenide fibers. *Journal of Lightwave Technology* **2017**, 35, 5397-5403. https://doi.org/10.1109/JLT.2017.2775864
73. Andrianov, A., Szabo, A., Sergeev, A., Kim, A., Chvykov, V., Kalashnikov, M. Computationally efficient method for Fourier transform of highly chirped pulses for laser and parametric amplifier modeling. *Opt. Express* **2016**, 24, 25974-25982. https://doi.org/10.1364/OE.24.025974
74. Gomes, L., Lousteau, J., Milanese, D., Scarpignato, G. C., Jackson, S. D. Energy transfer and energy level decay processes in Tm3+-doped tellurite glass. *J. Appl. Phys.* **2012**, 111, 063105. https://doi.org/10.1063/1.3694747
75. Ng, L.N., Taylor, E.R., Nilsson, J. 795 nm and 1064 nm dual pump thulium-doped tellurite fibre for S-band amplification. *Electron. Lett*. **2002**, 38, 1246-1247. https://doi.org/10.1049/el:20020883
76. Taylor, E. R. M., Ng, L. N., Nilsson, J., Caponi, R., Pagano, A., Potenza, M., Sordo, B. Thulium-doped tellurite fiber amplifier. *IEEE Photonics Technol. Lett*. **2004**, 16, 777-779. https://doi.org/10.1109/LPT.2004.823733
77. Caponi, R., Pagano, A., Potenza, M., Sordo, B., Taylor, E.M., Ng, L.N., Nilsson, J. and Poli, F. Nearly 10 dB net gain from a thulium-doped tellurite fibre amplifier over the S-band. ECOC-IOOC 2003 (29th European Conference on Optical Communication - 14th International Conference on Integrated Optics and Optical Fibre Communication). 21 - 25 Sep 2003.
78. Venkataiah, G., Babu, P., Martín, I. R., Krishnaiah, K. V., Suresh, K., Lavín, V., Jayasankar, C. K. Spectroscopic studies on Yb^{3+}-doped tungsten-tellurite glasses for laser applications. *Journal of Non-Crystalline Solids* **2018**, 479, 9-15. https://doi.org/10.1016/j.jnoncrysol.2017.09.036
79. Merzliakov, M. A., Kouhar, V. V., Malashkevich, G. E., Pestryakov, E. V. Spectroscopy of Yb-doped tungsten–tellurite glass and assessment of its lasing properties. *Optical Materials* **2018**, 75, 142-149. https://doi.org/10.1016/j.optmat.2017.10.018
80. Babu, A. M., Jamalaiah, B. C., Kumar, J. S., Sasikala, T., Moorthy, L. R. Spectroscopic and photoluminescence properties of Dy^{3+}-doped lead tungsten tellurite glasses for laser materials. *Journal of alloys and compounds* **2011**, 509, 457-462. https://doi.org/10.1016/j.jallcom.2010.09.058
81. Giridhar, P., Sailaja, S., Reddy, M. B., Raju, K. V., Raju, C. N., Reddy, B. S. Spectroscopic studies of RE^{3+} (RE= Eu, Tb, Sm & Dy): lithium lead boro tellurite glasses. *Ferroelectrics Letters* **2011**, 38, 1-10. https://doi.org/10.1080/07315171.2011.570173
82. Annapurna, K., Chakrabarti, R., Buddhudu, S. Absorption and emission spectral analysis of Pr^{3+}: tellurite glasses. *J Mater Sci* **2007, 42,** 6755–6761. https://doi.org/10.1007/s10853-006-1465-x

Peer-reviewed version available at Fibers 2020, 8, 30; doi:10.3390/fib8050030

83. Marek, Ł., Sobczyk, M. Spectroscopic investigations of Pr^{3+} ions in Na_2O-La_2O_3-ZnO-TeO_2 glasses. *Journal of Non-Crystalline Solids* **2018**, 487, 96-103. https://doi.org/10.1016/j.jnoncrysol.2018.02.005
84. Stambouli, W., Elhouichet, H., Gelloz, B., Férid, M. Optical and spectroscopic properties of Eu-doped tellurite glasses and glass ceramics. *Journal of luminescence* **2016**, 138, 201-208. https://doi.org/10.1016/j.jlumin.2016.04.027
85. Alvarez-Ramos, M. E., Alvarado-Rivera, J., Zayas, M. E., Caldiño, U., Hernández-Paredes, J. Yellow to orange-reddish glass phosphors: Sm^{3+}, Tb^{3+} and Sm^{3+}/Tb^{3+} in zinc tellurite-germanate glasses. *Optical Materials* **2018**, 75, 88-93. https://doi.org/10.1016/j.optmat.2017.09.033
86. Kumar, A., Rai, D. K., Rai, S. B. Optical properties of Sm3+ ions doped in tellurite glass. *Spectrochimica Acta Part A: Molecular and Biomolecular Spectroscopy* **2003**, 59, 917-925. https://doi.org/10.1016/S1386-1425(02)00282-2